

Supporting Information

Bimetallic Oxide $\text{Fe}_{1.89}\text{Mo}_{4.11}\text{O}_7$ Electrocatalyst with Highly Efficient Hydrogen Evolution Reaction Activity in Alkaline and Acidic Media

Zhaomin Hao,^a Shishuai Yang,^a Jingyang Niu,^a Zhiqiang Fang,^a Liangliang Liu,^b Qingsong Dong,^{*,a} Shuyan Song^c, and Yong Zhao^{*,b}

^aHenan Key Laboratory of Polyoxometalate Chemistry, College of Chemistry and Chemical Engineering, Henan University, Kaifeng, 475004, Henan Province, P. R. China

^bKey Lab for Special Functional Materials of Ministry of Education Collaborative Innovation Center of Nano Functional Materials and Applications, Henan University, Kaifeng, 475004, Henan Province, P. R. China

^cState Key Laboratory of Rare Earth Resource Utilization, Changchun Institute of Applied Chemistry, Chinese Academy of Sciences, Changchun 130022, P. R. China

* Correspondence authors: zmhao@henu.edu.cn, zhaoyong@henu.edu.cn

Experimental Section	3
Chemicals	3
Synthesis of precursors.....	3
Synthesis of MoO ₂ , Fe/MoO ₂ and Fe _{1.89} Mo _{4.11} O ₇ /MoO ₂	4
Characterization	5
Electrochemical characterization	5
Scheme S1 The synthesis route to prepare molybdenum-based nanomaterials	7
Figure S1 The thermogravimetric studies	7
Figure S2 The EDX elemental mapping images of Fe and Mo in Fe_{1.89}Mo_{4.11}O₇/MoO₂	8
Figure S3 FESEM images of MoO₂ and Fe/MoO₂	8
Figure S4 HRTEM image of Fe_{1.89}Mo_{4.11}O₇/MoO₂ sample	9
Figure S5 Polarization curves of Fe_{1.89}Mo_{4.11}O₇/MoO₂ with different loadings	9
Figure S6 Polarization curves of Fe_{1.89}Mo_{4.11}O₇/MoO₂ prepared with different annealing temperature	10
Figure S7 XRD patterns of Fe_{1.89}Mo_{4.11}O₇/MoO₂ prepared with different annealing temperature	10
Figure S8 The onset potential of Fe_{1.89}Mo_{4.11}O₇/MoO₂ catalyst in 1 M KOH	11
Figure S9 The onset potential of Fe_{1.89}Mo_{4.11}O₇/MoO₂ catalyst in 0.5 M H₂SO₄	11
Figure S10 The Tafel plots in 1 M KOH	12
Figure S11 The exchange current density of Fe_{1.89}Mo_{4.11}O₇/MoO₂ catalyst in 1 M KOH ...	12
Figure S12 The Tafel plots in 0.5 M H₂SO₄	13
Figure S13 The exchange current density of Fe_{1.89}Mo_{4.11}O₇/MoO₂ catalyst 0.5 M H₂SO₄ ..	13
Table S1 The HER performance of catalysts in this paper	14
Table S2 Comparison of HER performance for Fe_{1.89}Mo_{4.11}O₇/MoO₂ with other HER electrocatalysts	15
Figure S14 Polarization curves of Fe_{1.89}Mo_{4.11}O₇/MoO₂ after continuous potential sweeps at 20 mV s⁻¹	16
Figure S15 Time-dependent current density curves (carbon as a counter electrode) of the Fe_{1.89}Mo_{4.11}O₇/MoO₂ in 1 M KOH	16
Figure S16 The HRTEM images for Fe_{1.89}Mo_{4.11}O₇/MoO₂ in 1 M KOH and 0.5 M H₂SO₄ after 3000 potential sweeps	17
Figure S17 The DFT calculation of metal-hydrogen bond strength based on Mo and Fe element in Fe_{1.89}Mo_{4.11}O₇	17
Figure S18 Optimized structure of Fe_{1.89}Mo_{4.11}O₇/Fe_{1.89}Mo_{4.11}O₇-H, MoO₂/MoO₂-H, Mo₅O₁₄/Mo₅O₁₄-H and Mo₈O₂₃/Mo₈O₂₃-H	18

Experimental Section

Chemicals

All chemical reagents were used as received without further purification.

Synthesis of precursors

Ferrimolybdate: The solution of $\text{H}_3[\text{PMo}_{12}\text{O}_{40}]\cdot\text{XH}_2\text{O}$, 1,10-phen, Fe_2O_3 , NH_4VO_3 , triethylamine and distilled water in a molar ratio of 1 : 1.5 : 1 : 0.5 : 2 : 1000 was stirred for 1h, and the pH value of solution was adjusted to 5.0 by 2 mol L^{-1} HCl solution. The mixture was then transferred into a Teflon-lined autoclave reactor (20 mL) at 175 °C for 5 days. The reactor was slowly cooled to room temperature. The resulted red-black block crystals were filtered, washed with water, and dried at room temperature. Anal. Calcd: C, 21.19; H, 1.17; N, 4.12; Fe, 4.12. Found: C, 21.74; H, 1.76; N, 4.01; Fe, 4.08. The crystal structure of ferrimolybdate was checked by single crystal X-ray diffractometer before it was used as precursor.

Polymolybdate: $(\text{NH}_4)_6\text{Mo}_7\text{O}_{24}\cdot 4\text{H}_2\text{O}$, 1,10-phen, H_3PO_4 and distilled water in a molar ratio of 1 : 0.05 : 0.1 : 2 : 1000 were mixed. The resulting suspension was stirred for 30min and then was transferred into a Teflon-lined autoclave reactor (20 mL). After heating at 170 °C for 3 days, the reactor was slowly cooled to room temperature. Yellow block crystals were filtered, washed with water, and dried at room temperature. Anal. Calcd: C, 18.31; H, 1.08; N, 3.55. Found: C, 18.28; H, 1.17; N, 3.56. The crystal structure of ferrimolybdate was checked by single crystal X-ray diffractometer before it was used as precursor.

Synthesis of MoO₂, Fe/MoO₂ and Fe_{1.89}Mo_{4.11}O₇/MoO₂

MoO₂: 0.5 g polymolybdates powder was homogeneously dispersed in a ceramic boat that was then put into a tube furnace. The sample was annealed under a continuous nitrogen flux of 10 sccm at 1000 °C for 1 hour, and then the ceramic boat was slowly cooled to room temperature. After the annealing was completed, the powders were collected. The heat-treated MoO₂ was then pre-leached in 0.5 M H₂SO₄ at 40 °C for 8 hours to remove unstable and inactive species from the catalyst, and thoroughly washed in de-ionized water. Finally, the catalyst was heat-treated again at nitrogen-gas atmosphere for 1 hour to get the final MoO₂.

Fe/MoO₂: 0.5 g polymolybdates and 0.533 g Fe(NO₃)₃·9H₂O were homogeneously mixed and then dispersed in a ceramic boat. Next, the samples were annealed in a tube furnace under a continuous nitrogen flux of 10 sccm at 1000 °C for 1 hour, and then the ceramic boat was slowly cooled to room temperature. The heat-treated Fe/MoO₂ was then pre-leached in 0.5 M H₂SO₄ at 40 °C for 8 hours to remove unstable and inactive species from the catalyst, and thoroughly washed in de-ionized water. Finally, the catalyst was heat-treated again in nitrogen-gas atmosphere for 1 hour to get the final Fe/MoO₂.

Fe_{1.89}Mo_{4.11}O₇/MoO₂: 0.5 g Ferrimolybdate powder was homogeneously dispersed in a ceramic boat that was then put into a tube furnace. The samples were annealed under a continuous nitrogen flux of 10 sccm at 1000 °C for 1 hour, and then the ceramic boat was slowly cooled to room temperature. After the annealing was completed, the powders were collected. The heat-treated Fe_{1.89}Mo_{4.11}O₇/MoO₂ was then pre-leached in 0.5 M H₂SO₄ at 40 °C for 8 hours to remove unstable and inactive species from the catalyst, and thoroughly washed in de-ionized water. Finally, the catalyst was heat-treated again in nitrogen-gas atmosphere for 1 hour to get the final Fe_{1.89}Mo_{4.11}O₇/MoO₂.

Characterization

Powder X-ray diffraction (XRD) measurement was performed on a Bruker D8 Focus Powder X-ray diffractometer using Cu K α ($\lambda = 0.15405$ nm) radiation (40 kV, 40 mA). X-ray photoelectron spectra (XPS) was measured with VG ESCALAB MK (VK Company, UK) at room temperature by using a Al K α X-ray source at 12 KV and 20 mA. The morphology of the nickel sulfide was analyzed by on a JSM-6701Feld-emission scanning electron microscope (FE-SEM) with 10KV and 10mA. Energy dispersive spectroscopy (EDS) data was collected with an ensemble measurement in the FE-SEM. Transmission electron microscope (TEM) was performed using a FEI Tecnai G2 S-Twin instrument with a field emission gun operating at 200 kV. Nitrogen adsorption measurements were performed on a Micromeritics ASAP 2020 adsorption analyzer. Specific surface areas were calculated by the Brunauer-Emmert-Teller method. Mass analysis of the generated gases was performed using an Ominstar-Thermostar GSD 320 system (Pfeiffer Vacuum) mass spectrometer, wherein argon gas was chosen as carrier gas. The electrochemical experiments were carried out with a ModuLab XM electrochemical workstation (Solartron Analytical, UK).

Electrochemical characterization

Electrochemical measurements were performed at room temperature in a standard three-electrode system. A platinum gauze electrode and a saturated calomel electrode (SCE) served as the counter electrode and the reference electrode, respectively. The preparation of working electrode was described with the following procedures: 5 mg of catalyst powder was dispersed in diluted Nafion alcohol solution containing 1 mL ethanol and 50 μ L Nafion, and then ultrasonicated for 2 h to obtain a homogeneous suspension. Next, the suspension was homogeneously loaded on a bare carbon paste and dried at room temperature. Potentials were referenced to a reversible hydrogen electrode (RHE): $E(\text{RHE}) = E(\text{SCE}) + 0.242 + 0.059 \times$

*p*H. Linear sweep voltammetry (LSV) was recorded in 1.0 M KOH and 0.5 M H₂SO₄ at a scan rate of 5 mV s⁻¹ to obtain the polarization curves. The long-term stability tests were performed by continuous LSV scans at a sweep rate of 20 mV s⁻¹.

Scheme S1 The synthesis route to prepare molybdenum-based nanomaterials

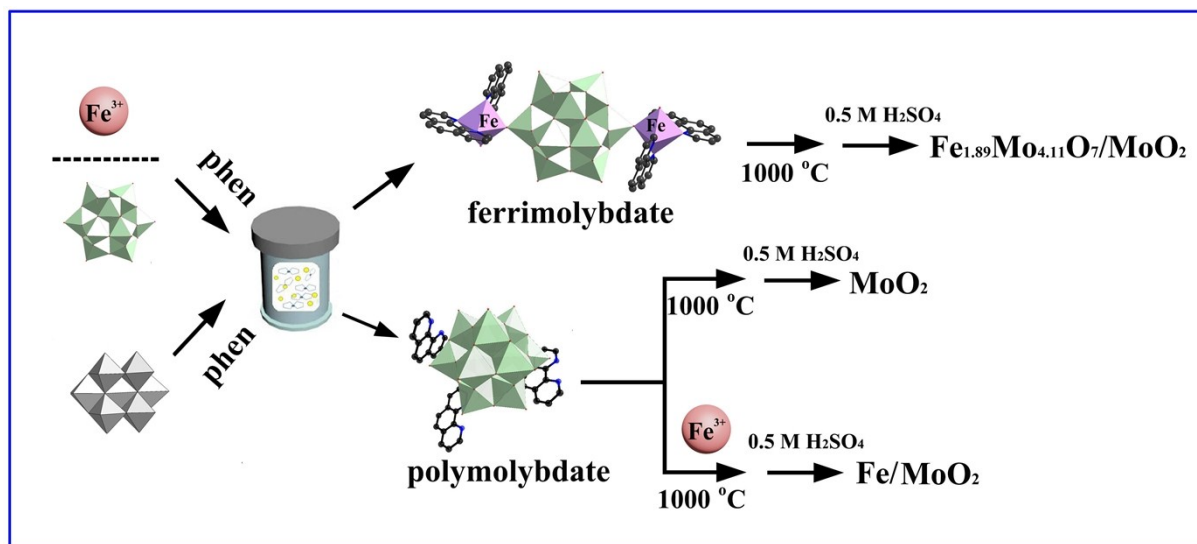


Figure S1 The thermogravimetric studies: CO_2 signals detected by mass spectrum during the thermal treatment of ferrimolybdate, polymolybdates and polymolybdates + Fe^{3+}

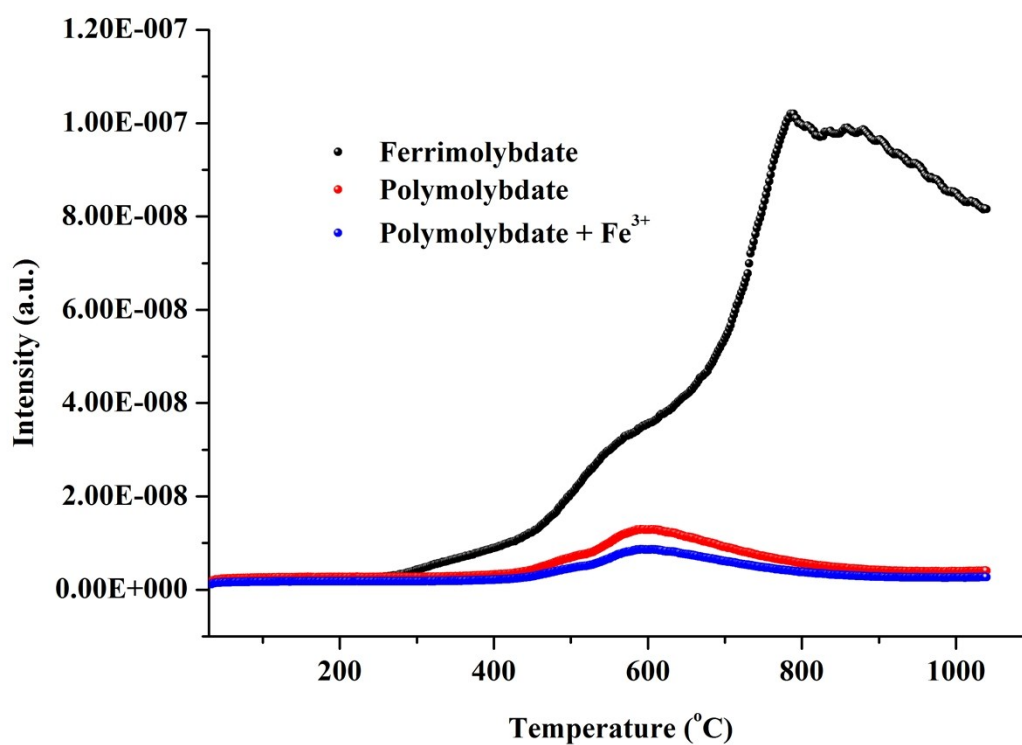


Figure S2 The EDX elemental mapping images of Fe and Mo in

$\text{Fe}_{1.89}\text{Mo}_{4.11}\text{O}_7/\text{MoO}_2$

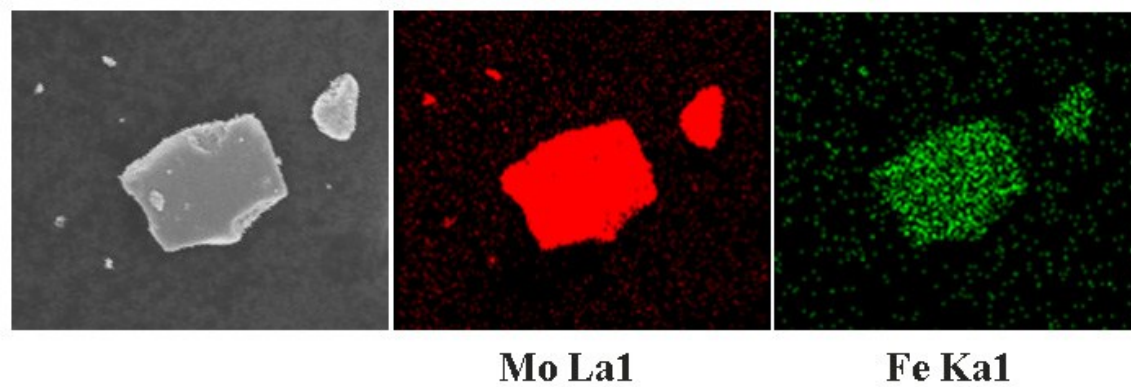


Figure S3 FESEM images of MoO_2 and Fe/MoO_2 for a) precursors of MoO_2 , b) precursors of Fe/MoO_2 , c) final products of MoO_2 , d) final products of Fe/MoO_2 .

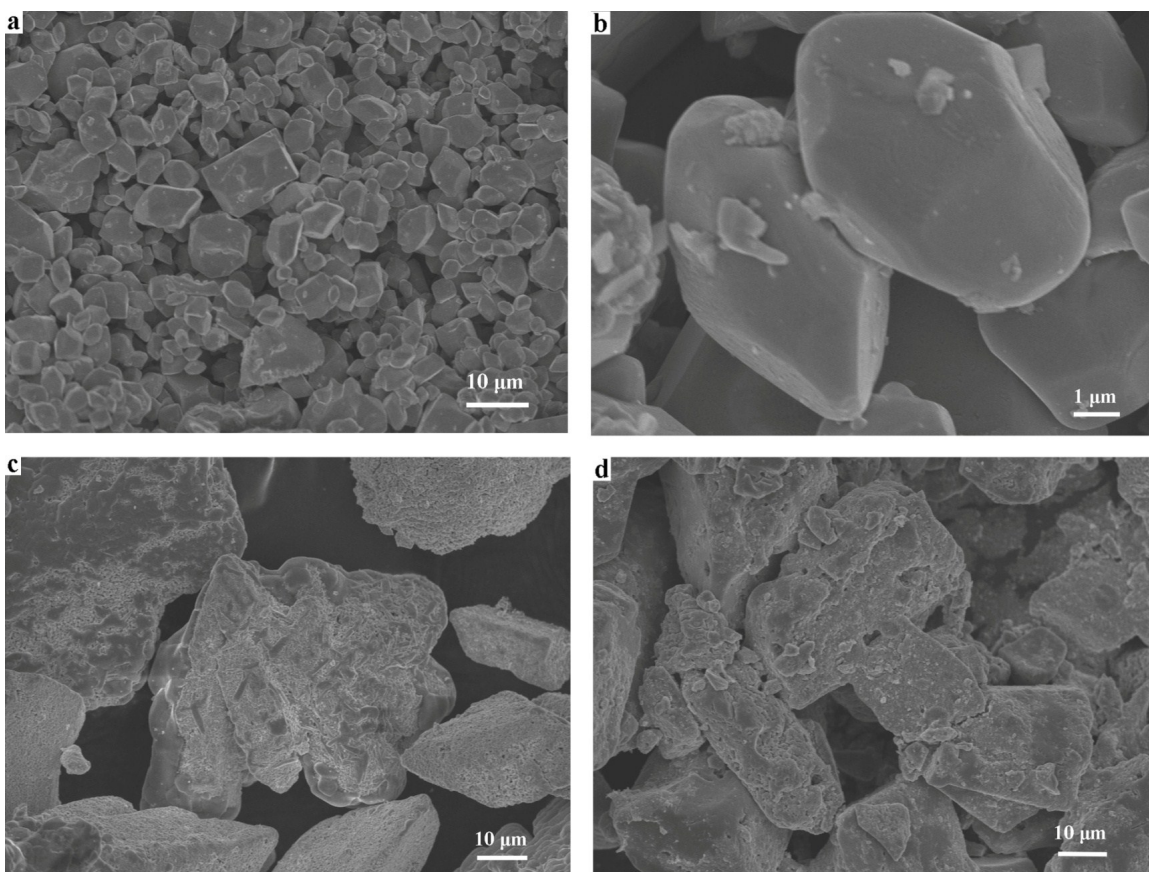


Figure S4 HRTEM image of $\text{Fe}_{1.89}\text{Mo}_{4.11}\text{O}_7/\text{MoO}_2$ sample.

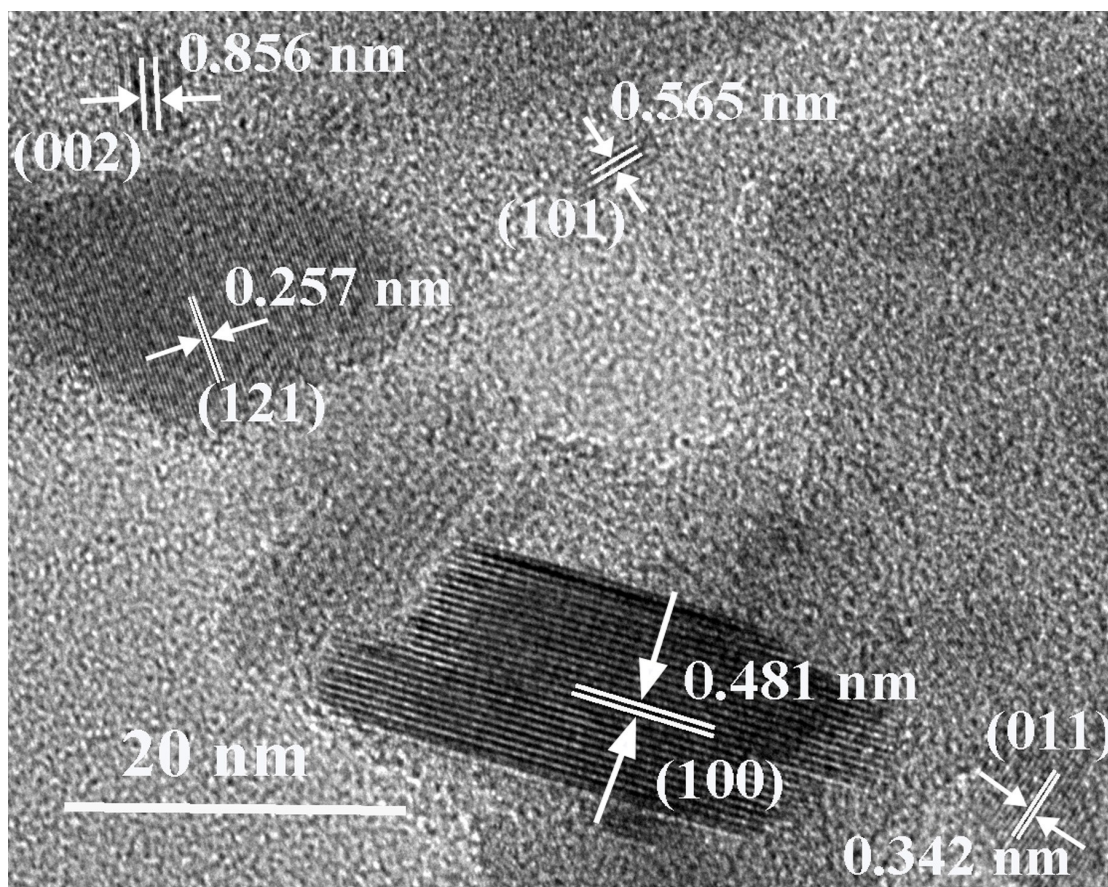


Figure S5 Polarization curves of $\text{Fe}_{1.89}\text{Mo}_{4.11}\text{O}_7/\text{MoO}_2$ with different loadings.

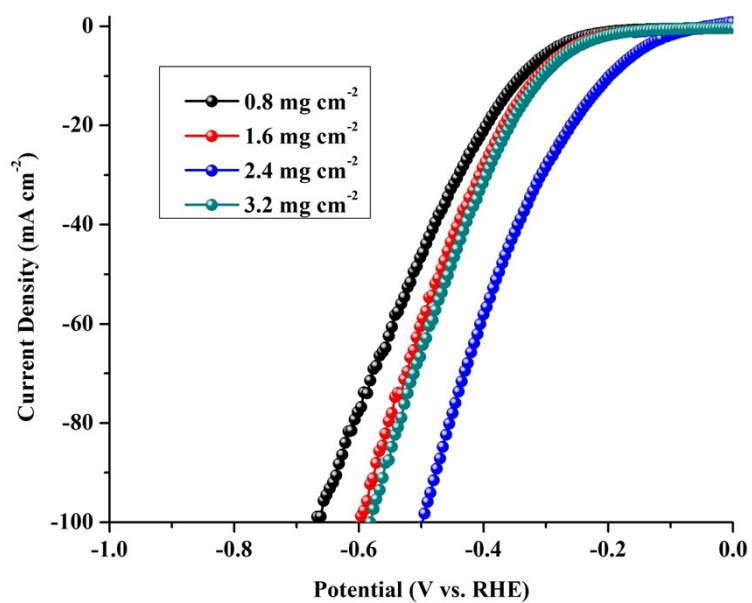


Figure S6 Polarization curves of $\text{Fe}_{1.89}\text{Mo}_{4.11}\text{O}_7/\text{MoO}_2$ prepared with different annealing temperature.

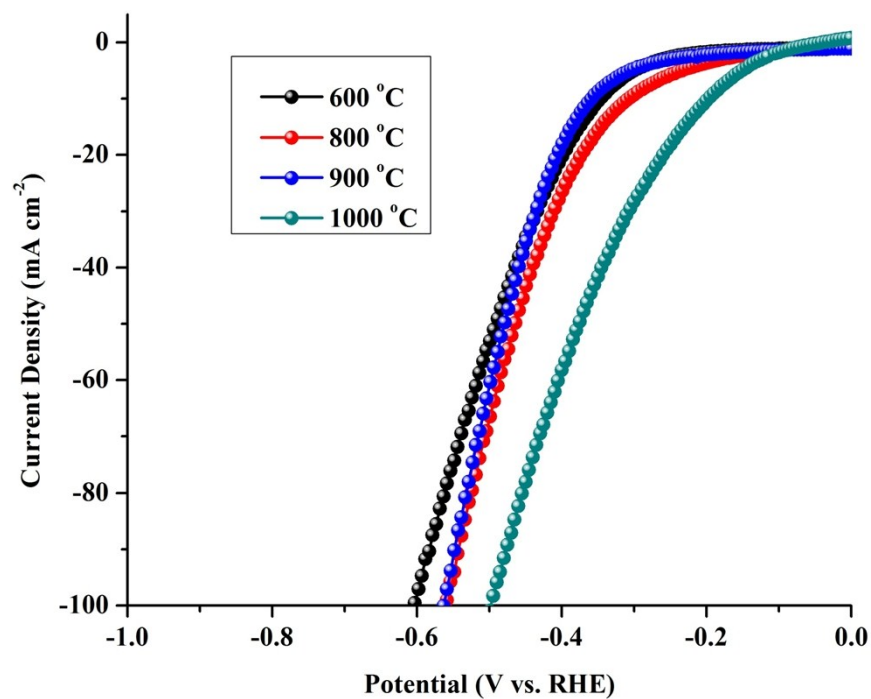


Figure S7 XRD patterns of $\text{Fe}_{1.89}\text{Mo}_{4.11}\text{O}_7/\text{MoO}_2$ prepared with different annealing temperature.

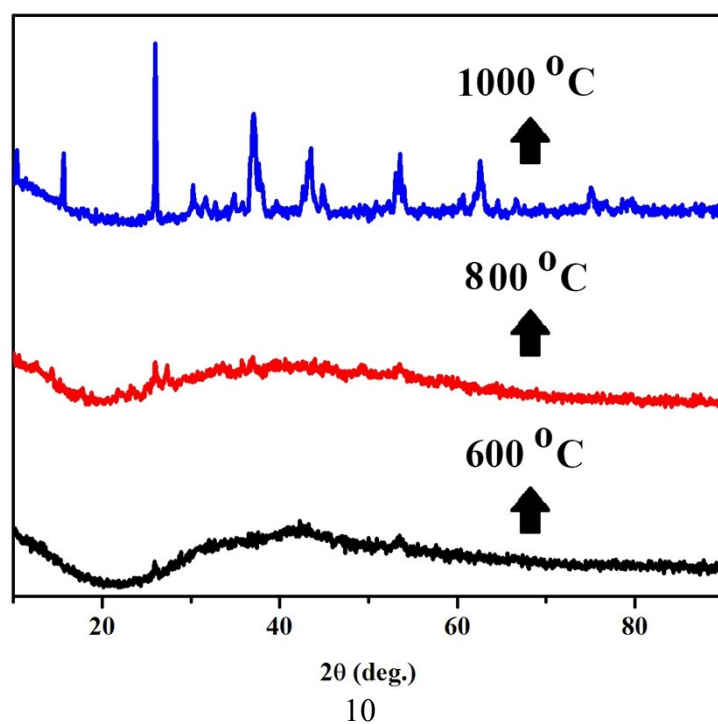


Figure S8 The onset potential of $\text{Fe}_{1.89}\text{Mo}_{4.11}\text{O}_7/\text{MoO}_2$ catalyst in 1 M KOH

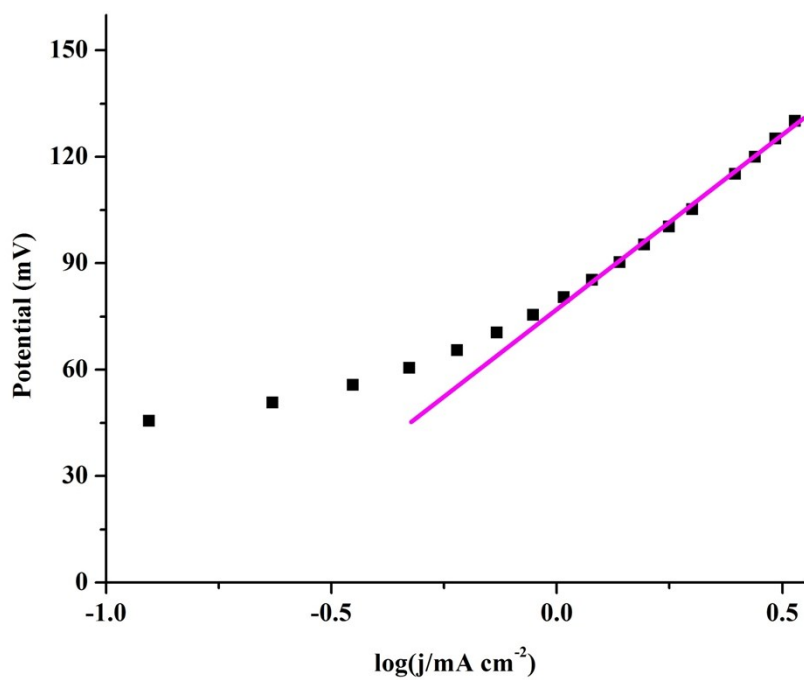


Figure S9 The onset potential of $\text{Fe}_{1.89}\text{Mo}_{4.11}\text{O}_7/\text{MoO}_2$ catalyst in 0.5 M H_2SO_4

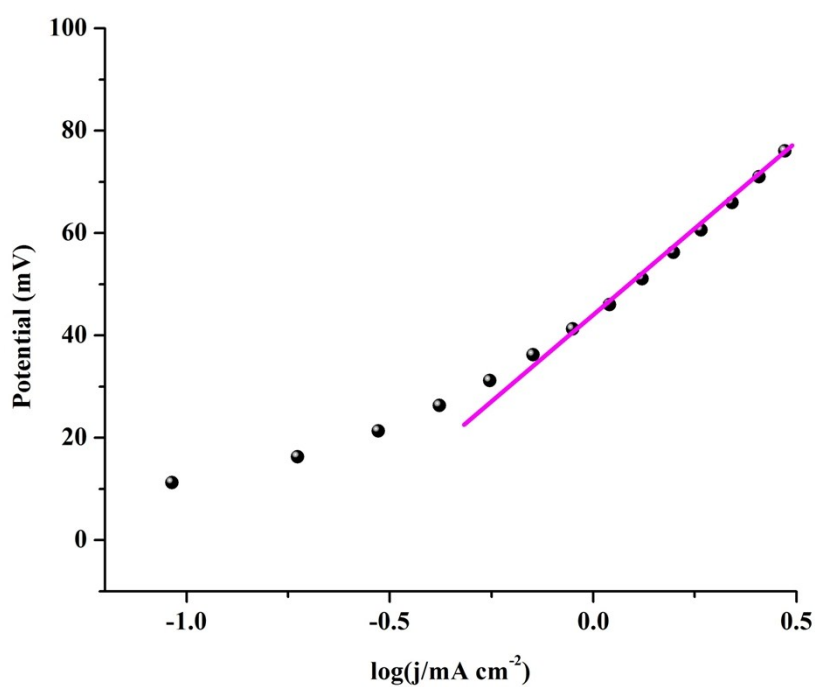


Figure S10 The Tafel plots in 1 M KOH

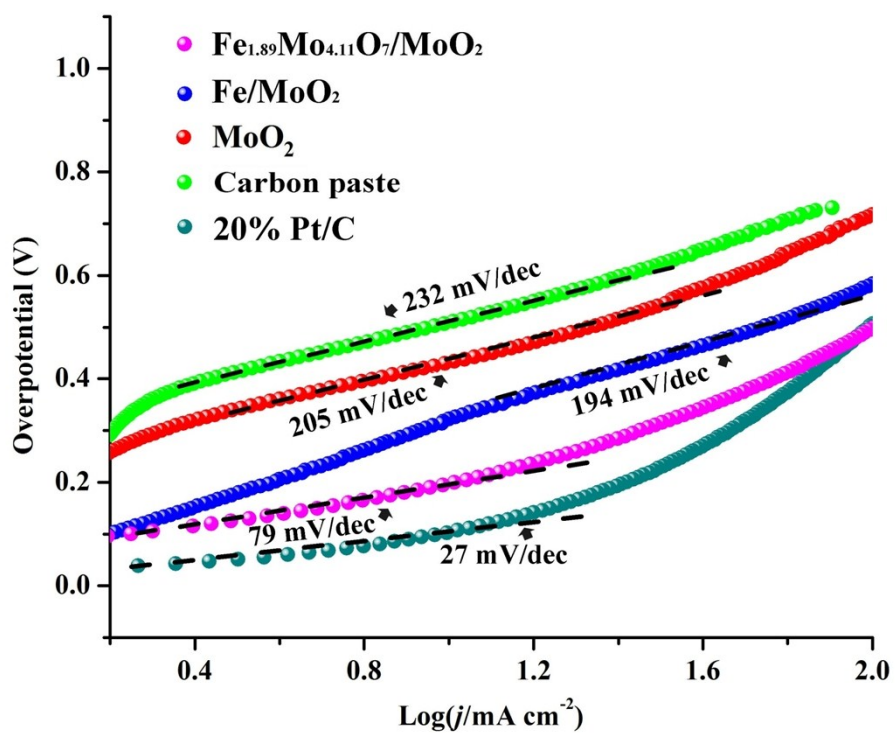


Figure S11 The exchange current density of $\text{Fe}_{1.89}\text{Mo}_{4.11}\text{O}_7/\text{MoO}_2$ catalyst in 1 M KOH

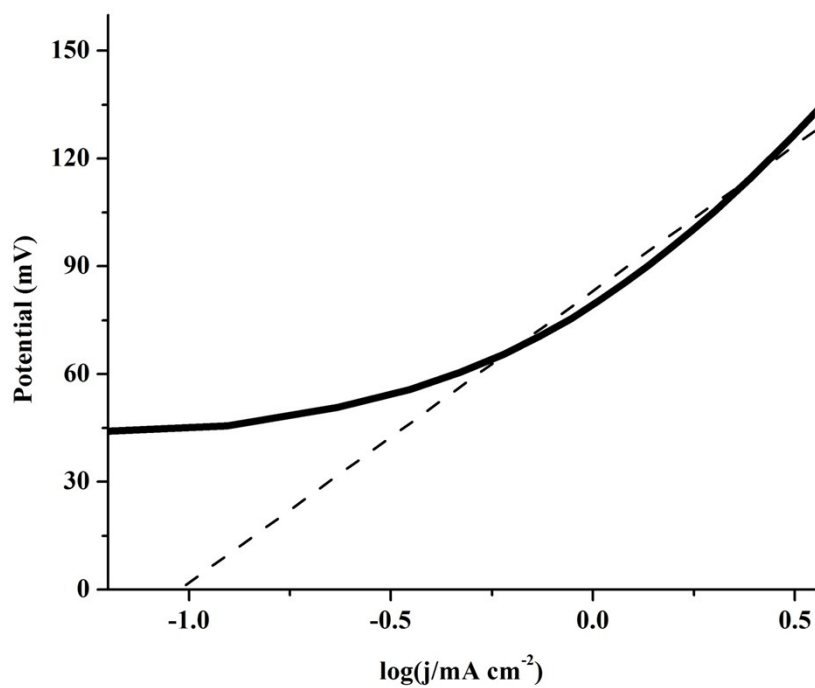


Figure S12 The Tafel plots in 0.5 M H₂SO₄

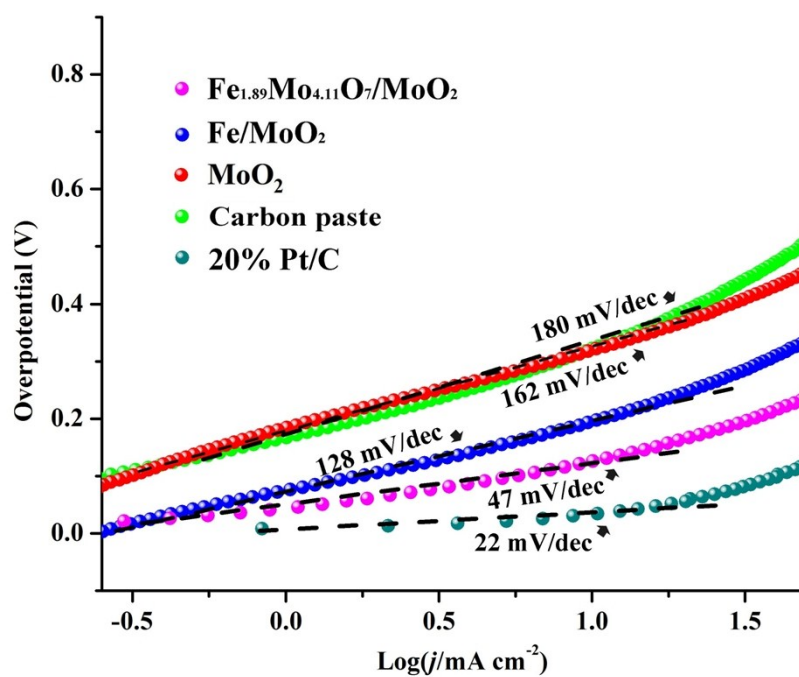


Figure S13 The exchange current density of Fe_{1.89}Mo_{4.11}O₇/MoO₂ catalyst

0.5 M H₂SO₄

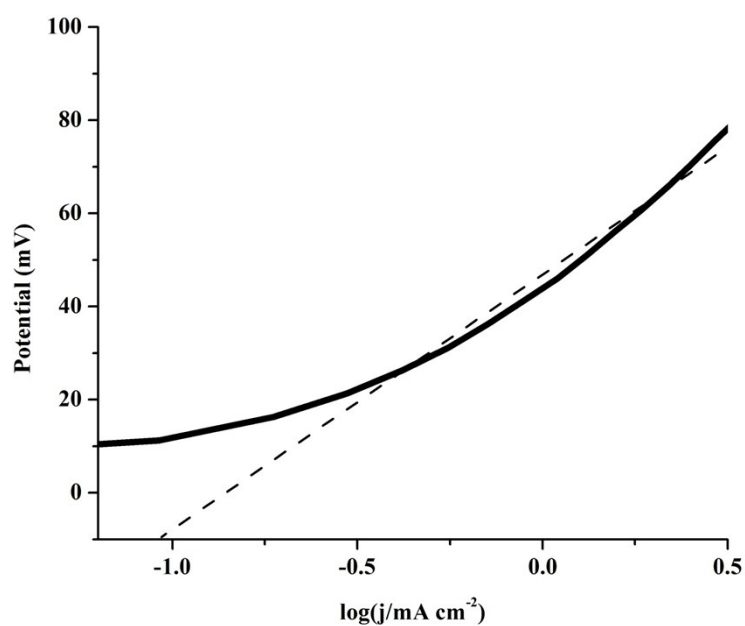


Table S1 The HER performance of catalysts in this paper

Samples	Electrolyte	Tafel slope (mV dec ⁻¹)	η (mV) at 10 mA cm ⁻²
Carbon paste	1 M KOH	232	514
	0.5 M H ₂ SO ₄	180	321
20% Pt/C	1 M KOH	27	103
	0.5 M H ₂ SO ₄	22	33
MoO ₂	1 M KOH	205	431
	0.5 M H ₂ SO ₄	162	318
Fe/MoO ₂	1 M KOH	194	322
	0.5 M H ₂ SO ₄	128	194
Fe _{1.89} Mo _{4.11} O ₇ /MoO ₂	1 M KOH	79	197
	0.5 M H ₂ SO ₄	47	125

Table S2 Comparison of HER performance for Fe_{1.89}Mo_{4.11}O₇/MoO₂ with other HER electrocatalysts

Samples	Electrolyte	Onset η (mV)	Tafel slope (mV dec ⁻¹)	η (mV) at 10 mA cm ⁻²	Ref.
Double-gyroid MoS ₂ /FTO	0.5 M H ₂ SO ₄	200–150	50	240	<i>Nat. Mater.</i> 2012 , <i>11</i> , 963
MoS ₂ /CoSe ₂ hybrid	0.5 M H ₂ SO ₄	11	36	68	<i>Nat. Commun.</i> 2015 , <i>6</i> , 5982
Exfoliated metallic MoS ₂ nanosheets	0.1 M H ₂ SO ₄	135	43	187	<i>Nat. Mater.</i> 2013 , <i>12</i> , 850.
MoO ₃ -MoS ₂	0.5 M H ₂ SO ₄	200	50-60	250	<i>Nano Lett.</i> 2011 , <i>11</i> , 4168
NiMoN _x /C	0.1 M HClO ₄	78	35.9	170	<i>Angew. Chem. Int. Ed.</i> 2012 , <i>51</i> , 6131
MoS ₂ /RGO	0.5 M H ₂ SO ₄	100	41	140	<i>J. Am. Chem. Soc.</i> 2011 , <i>133</i> , 7296.
MoO ₂ /MoSe ₂	0.5 M H ₂ SO ₄	63	49.1	181	<i>Adv. Funct. Mater.</i> 2016 , <i>26</i> , 8537
MoSe ₂ /Mo	0.5 M H ₂ SO ₄	89	34.7	166	<i>Adv. Mater.</i> 2016 , <i>28</i> , 9831.
Co-Mo-S _x	0.1 M KOH			>200	<i>Nat. Mater.</i> 2016 , <i>15</i> , 197
	0.1 M HClO ₄			>200	
Fe _{1.89} Mo _{4.11} O ₇ /MoO ₂	1 M KOH	70	79	197	This work
	0.5 M H ₂ SO ₄	40	47	125	

Figure S14 Polarization curves of $\text{Fe}_{1.89}\text{Mo}_{4.11}\text{O}_7/\text{MoO}_2$ after continuous potential sweeps at 20 mV s^{-1}

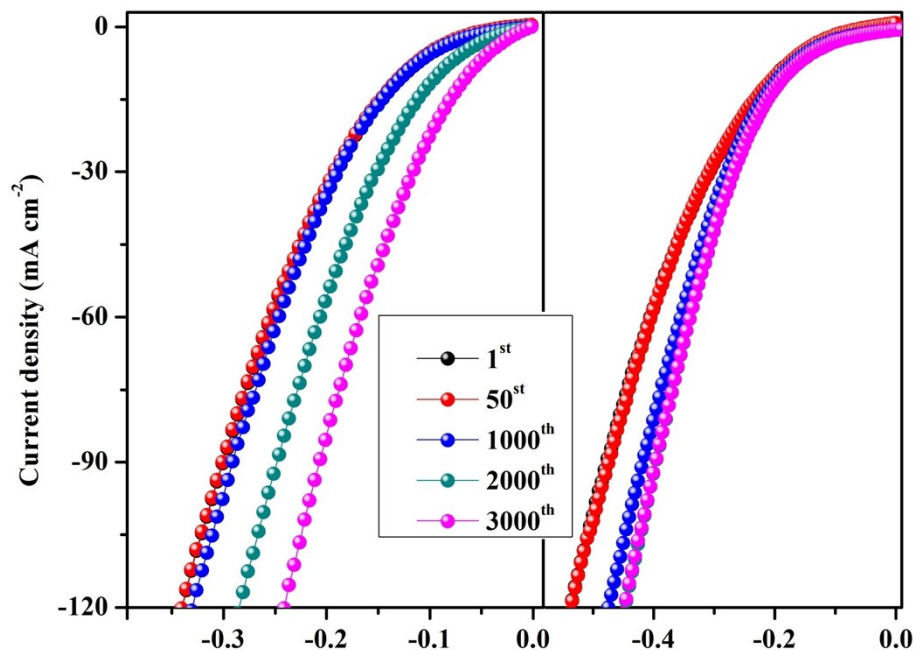


Figure S15 Time-dependent current density curves (carbon as a counter electrode) of the $\text{Fe}_{1.89}\text{Mo}_{4.11}\text{O}_7/\text{MoO}_2$ in 1 M KOH

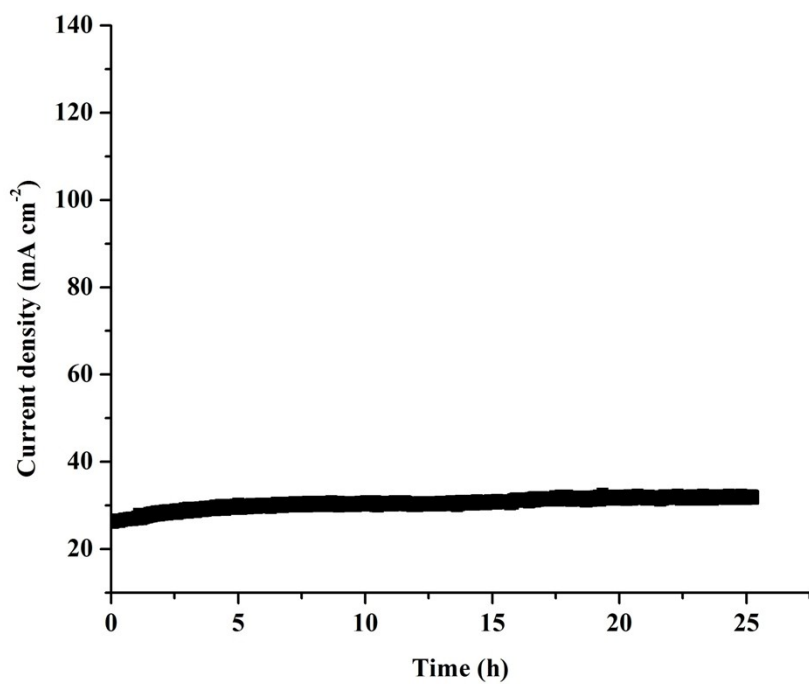


Figure S16 The HRTEM images for $\text{Fe}_{1.89}\text{Mo}_{4.11}\text{O}_7/\text{MoO}_2$ in 1 M KOH and 0.5 M H_2SO_4 after 3000 potential sweeps

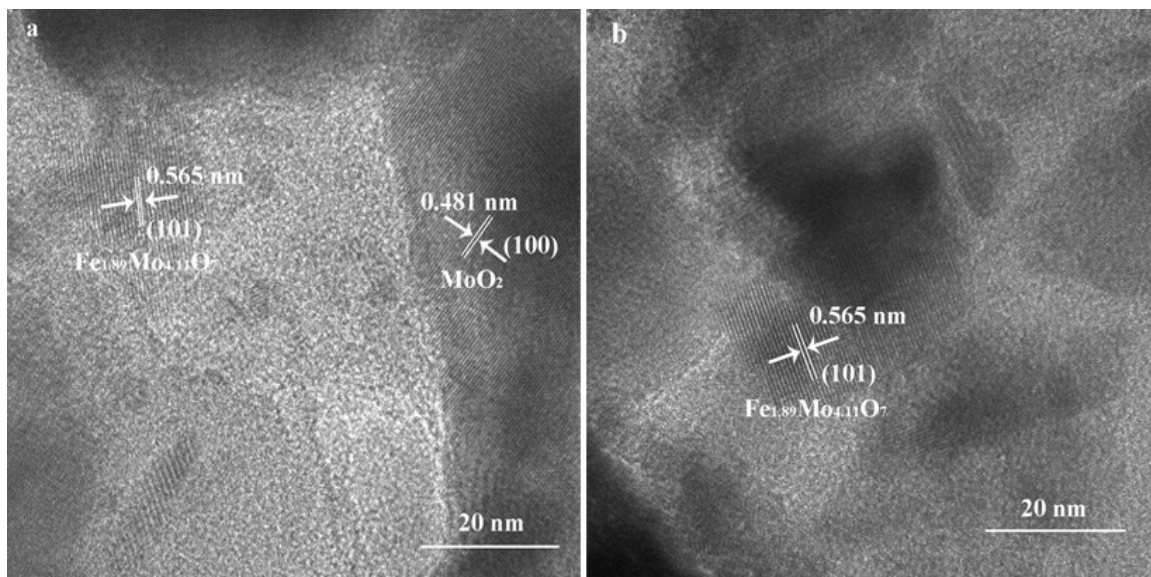
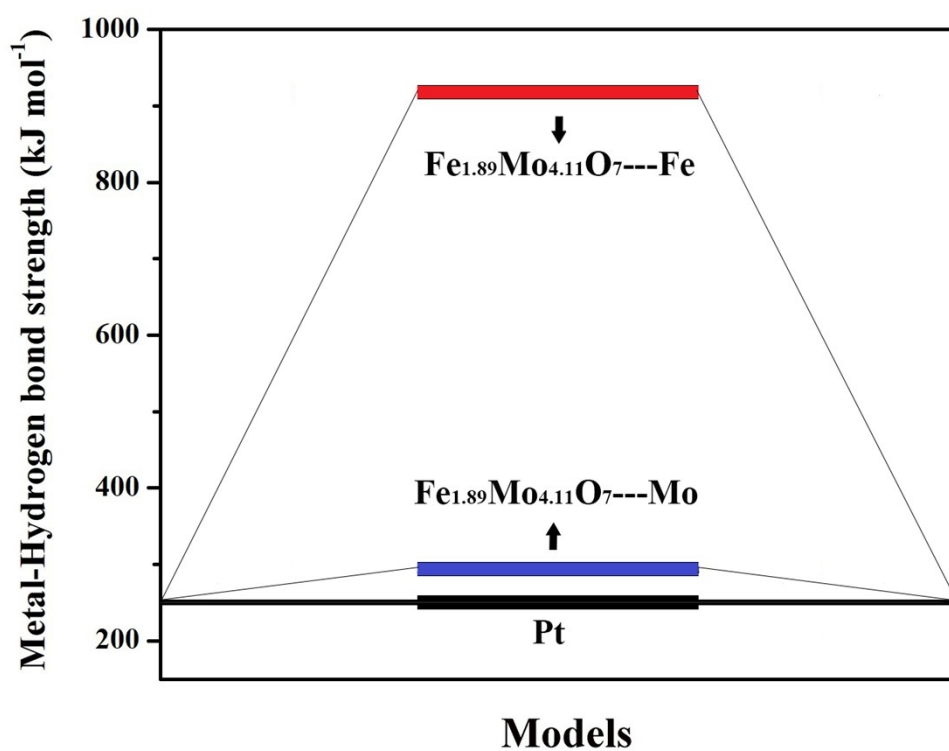


Figure S17 The DFT calculation of metal-hydrogen bond strength based on Mo and Fe element in $\text{Fe}_{1.89}\text{Mo}_{4.11}\text{O}_7$.



**Figure S18 Optimized structure of $\text{Fe}_{1.89}\text{Mo}_{4.11}\text{O}_7/\text{Fe}_{1.89}\text{Mo}_{4.11}\text{O}_7\text{-H}$, MoO_2
/ $\text{MoO}_2\text{-H}$, $\text{Mo}_5\text{O}_{14}/\text{Mo}_5\text{O}_{14}\text{-H}$ and $\text{Mo}_8\text{O}_{23}/\text{Mo}_8\text{O}_{23}\text{-H}$.**

We perform DFT calculation using the Vienna Ab Initio Simulation Package (VASP), the Perdew-Becke-Ernzerhof (PBE) is used for the exchange-correlation functional. The cut-off energies for plane waves is 450 eV, providing a convergence of 10^{-4} eV in total energy and 0.02 eV/Å in Hellmann Feynman force on each atom. The metal-hydrogen bond strength in $\text{Fe}_{1.89}\text{Mo}_{4.11}\text{O}_7$ is calculated to state the Mo active sites with MoO_2 , Mo_5O_{14} and Mo_8O_{23} . All adsorption sites were based on Mo for comparison, and all initial structures and optimized intermediates were listed as following.

